

PROCEEDINGS OF SPIE

SPIDigitalLibrary.org/conference-proceedings-of-spie

Voltage dependence of retardance, flicker, and director angle orientation in reflective liquid crystal devices by average Stokes polarimetry

Andrés Márquez, Francisco Martínez-Guardiola, Marta Morales-Vidal, Daniel Puerto, Jorge Francés, et al.

Andrés Márquez, Francisco J. Martínez-Guardiola, Marta Morales-Vidal, Daniel Puerto, Jorge Francés, Sergi Gallego, Inmaculada Pascual, Augusto Beléndez, "Voltage dependence of retardance, flicker, and director angle orientation in reflective liquid crystal devices by average Stokes polarimetry," Proc. SPIE 11841, Optics and Photonics for Information Processing XV, 1184108 (1 August 2021); doi: 10.1117/12.2595742

SPIE.

Event: SPIE Optical Engineering + Applications, 2021, San Diego, California, United States

Voltage dependence of retardance, flicker and director angle orientation in reflective liquid crystal devices by average Stokes polarimetry

Andrés Márquez^{1,2}, Francisco J. Martínez-Guardiola^{1,2}, Marta Morales-Vidal², Daniel Puerto^{1,2}, Jorge Francés^{1,2}, Sergi Gallego^{1,2}, Inmaculada Pascual^{2,3}, Augusto Beléndez^{1,2}

¹Dept. de Física, Ing. de Sistemas y T. Señal, Universidad de Alicante, P.O. Box 99, E-03080, Alicante, Spain

²I.U. Física Aplicada a las Ciencias y las Tecnologías U. de Alicante, P.O. Box 99, E-03080, Alicante, Spain

³Dept. de Óptica, Farmacología y Anatomía, Univ. de Alicante, P.O. Box 99, E-03080, Alicante, Spain

ABSTRACT

Parallel-aligned liquid crystal on silicon devices (PA-LCoS) can be found nowadays in most of the advanced areas in optics and photonics. Many works have been dedicated to their characterization for optimum utilization in applications. However, usual techniques are based on diffractive or interferometric measurements. Recently, we proposed the use of Stokes polarimetry for a versatile yet easy to implement characterization. We show that the LCoS can be modelled as a non-absorbent reciprocal device which, combined with time-average Stokes polarimetry, enables to demonstrate robust measurements across the whole applied voltage range for the retardance and its flicker. One of the main novelties is that we also obtain the director orientation, which we show that changes across the voltage range, especially at larger applied voltages. This might affect in very sensitive applications. It might also provide a deeper insight into the internal dynamics in the LC layer.

Keywords: Polarization, Liquid crystal on silicon displays, Polarimetry, Spatial light modulation, Flicker, Liquid crystal director, Displays.

1. INTRODUCTION

The widespread use of parallel-aligned liquid crystal on silicon (PA-LCoS) microdisplays in modern spatial light modulation applications^{[1]-[3]} in optics and photonics, has stimulated the development of models and characterization techniques by many groups. These techniques can be generally classified as diffractive, interferometric and polarimetric^{[4]-[11]}. We have found specially interesting techniques based on the polarimetric approach. In this sense, when compared with other techniques, Stokes polarimetry represents a very simple yet robust approach, based on an analytical expression which makes it an easy and accurate technique.

PA-LCoS microdisplays can be easily modeled as a variable linear retarder, however, the existence of flicker^[12] and some other degradation phenomena such as cross-talk and fringing-field effects^{[13][14]} in many of these devices has resulted in the proposal of more complete models and characterization methods. In our group we have developed a series of polarimetric approaches. An analytical approach, simpler but limited, is the extended linear polarimeter^[8] to obtain the flicker at some retardance values. An alternative option, also analytical, is the use of a Stokes polarimeter, which we have used applying the time-average Stokes polarimetry technique^{[9][10]} to obtain both the linear retardance and its flicker at every applied voltage. Combined with a commercial Stokes polarimeter, this technique is a very fast and easy way to characterize the LCoS device. This was further applied with a semiphysical model able to calculate the tilt angle of the LC molecules in the LCoS and their fluctuations^[11], enabling to predict the linear retardance and its flicker for the whole visible wavelength range and for an incidence angle range from 0° to 45°. The applicability of this semiphysical approach for polarization state generation was also demonstrated^[11].

Usually, the director orientation of the PA-LCoS device needs to be found in advance to proceeding with the characterization technique of choice, be it diffractive, interferometric or polarimetric. This is done by inserting the LCoS between two crossed polarizers. The two crossed polarizers are rotated synchronously and, in the moment, when an

intensity null is obtained, then we know that the orientation of the neutral lines in the PA-LCoS device is coincident with the orientation of the transmission and extinction axis of the polarizers. This is a simple technique, typically used with conventional retarders, but requires additional manipulation and it would be more optimal if the director axis can be obtained in the same experiment considered for the average retardance and its flicker. Furthermore, we have found that when the LCoS is switched on, there are slight differences in the orientation of the crossed polarizers producing the intensity null as a function the applied voltage. To solve these situations recently we proposed a more general approach enabling to obtain the director orientation as a function of the applied voltage at the same time as the retardance and its flicker^[15]. In this work we show the new approach and demonstrate its accuracy comparing the theoretical predictions it provides with experimental measurements both in polarization state generation and in intensity modulation experiments.

2. THEORY

We give a brief review the theoretical development demonstrated in [15]. The departing point for our novel approach is to consider liquid-crystal spatial light modulators (LC-SLM), and PA-LCoS among them, as non-absorbent polarization elements. This is true in the sense that light loss is not dependent on the incident polarization or on the applied voltage, thus it can be factored out as a multiplicative scalar constant and the matrix describing the LC-SLM is a unitary matrix^{[16][17]}. Thus, the LC-SLM can be described as an equivalent rotated linear retarder. In addition, they are reciprocal devices^{[16][17]}. Then, we consider the matrix representation for a reflective device which is non-absorbent and reciprocal, as it happens in general with LC devices. Here we provide the final expression calculated in [15] for the matrix M_{ref} of a reflective LC device,

$$M_{ref} = JR(-\theta)M_R(2\Gamma)R(\theta), \quad (1)$$

where J is the inversion matrix, $R(\theta)$ is the rotation matrix and $M_R(\Gamma)$ is the unrotated linear retarder matrix for a retardance Γ , where we consider the fast axis along the x axis. We use a right-handed reference system, where the x and y axis are respectively along the vertical and horizontal directions of the lab, with the z axis along the direction of propagation of the light. We apply the Mueller-Stokes formalism^[18] since it allows to consider the existence of depolarized light. We see that Eq. (1) expresses that the action of a reflective LC device is equivalent to that of a rotated linear retarder.

A simple Stokes vector expression for the output state of polarization (SOP) is produced when illuminating the device with circularly polarized light. For example, for right-handed circular (RHC) light, i.e. ($S_0=I_0$, $S_1=0$, $S_2=0$, $S_3=I_0$), with I_0 the incident intensity, the output SOP is:

$$\vec{S}_{out} = I_0 \begin{pmatrix} 1 \\ -\sin(\Gamma)\sin(2\theta) \\ -\sin(\Gamma)\cos(2\theta) \\ -\cos(\Gamma) \end{pmatrix}. \quad (2)$$

To incorporate the existence of fluctuations let us consider a triangular profile for the variation of retardance with time $\Gamma(t)$ as in [9][10]. Typically, fluctuations are considerably faster than the integration time of detector systems, thus the expression of interest many times is the averaged output Stokes vector. Thus, we calculate the average values for the cosine and the sine functions in Eq. (2),

$$\langle \vec{S}_{out} \rangle = I_0 \begin{pmatrix} 1 \\ -\text{sinc}(a)\sin(\bar{\Gamma})\sin(2\theta) \\ -\text{sinc}(a)\sin(\bar{\Gamma})\cos(2\theta) \\ -\text{sinc}(a)\cos(\bar{\Gamma}) \end{pmatrix}, \quad (3)$$

where $\text{sinc}(a) \equiv \sin(a)/a$, and $\bar{\Gamma}$ and a are respectively the values for the average retardance and its fluctuation amplitude.

This provides an analytical strategy to calculate the three parameters in the model, as follows,

$$tg(\bar{\Gamma}) = \sqrt{\langle S_1 \rangle^2 + \langle S_2 \rangle^2} / \langle S_3 \rangle \quad (4a)$$

$$sinc(a) = \sqrt{\langle S_1 \rangle^2 + \langle S_2 \rangle^2 + \langle S_3 \rangle^2} / \langle S_0 \rangle \quad (4b)$$

$$tg(2\theta) = \langle S_1 \rangle / \langle S_2 \rangle \quad (4c)$$

, where $\langle S_0 \rangle$, $\langle S_1 \rangle$, $\langle S_2 \rangle$ and $\langle S_3 \rangle$ are the components of the Stokes vector. In particular, the result in Eq. (4b) corresponds to the degree of polarization (DoP) of the light reflected by the LCoS.

Then, as whole our procedure generates a very easy matrix representation with just three parameters to be characterized in the case of reflective devices. These parameters are the linear retardance, the angle of orientation of the equivalent retarder, and in the case of existence of flicker, the flicker magnitude. We note that this is general for any reflective LC-SLM, for example twisted-nematic are also included. This approach can be very useful for PA-LCoS devices when the LC-director is not known. Even if it is known as a first approximation, we can measure if there are variations with the applied voltage, as we have already shown^[15]. This leads to a deeper insight into the dynamics of the LC layer, to more precise characterization and therefore a better predictive capability of the performance of the device in applications.

3. EXPERIMENT

For the experiments, the reflective liquid crystal device considered is a commercial PA-LCoS display, with 1920x1080 pixels and 0.7" diagonal. As shown in Fig. 1, we illuminate the device with the unexpanded beam of a 532 nm diode pumped solid state laser (CPS532 laser diode module from Thorlabs). To produce the incident RHC polarized light we consider a linear polarizer with its transmission axis at -45° from the fast axis of a quarter-wave retarder. The light is quasiperpendicularly incident, at an angle of 5° to the normal of the LCoS entrance face. The SOP of the reflected beam is measured by the PAX5710VIS-T from Thorlabs. We enlarge the measurement time interval to obtain a time averaged signal which is representative of the time-varying SOP generated by the fluctuations in the device. To this goal, the time period (frequency) for the fluctuations in our PA-LCoS device is 8.66 ms (120 Hz). And the polarimeter averaging time considered in the paper, 600 ms, is much larger than actually needed to obtain fully stable and repeatable SOP measurements^{[9][10]}.

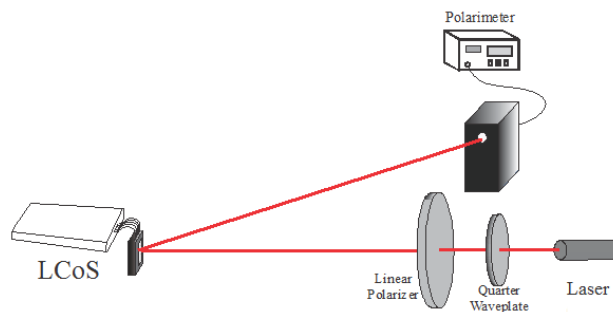


Fig. 1. Experimental setup used to measure linear retardance and flicker with the averaging Stokes polarimetric technique: quasi-perpendicular incidence at 5° with RHC state of polarization.

The LCoS device is digitally addressed^[10]. We consider the 5_6 sequence format, available in the vendor software, where the first number indicates the quantity of “equally weighted” bit-planes, and the second number the quantity of “binary” bit-planes^[9]. This sequence enables a large number of addressing levels, $(5+1) \times 2^6=384$ levels, with a reasonably low flicker magnitude. We also set the two levels of the binary voltage signal across the LC layer. The high and the low values are respectively the bright V_b and the dark V_d voltages in the vendor software. We set this values in this paper as $V_d=0.51V$ and $V_b=2.50V$, since they provide a good trade-off^[15] between large dynamic retardance range and not a large flicker magnitude.

4. RESULTS

4.1. Calibration of the parameters in the model

To show the possibility to measure the director orientation, together with the average retardance and its flicker, as a function of the applied voltage, we consider two orientations for the LCoS, shown in Fig. 2(a) and (c), respectively for the rows along the horizontal of the lab and rotated a certain angle. In Fig. 2(b) and (d) we present the values for the four Stokes components and for the resultant DoP, measured as a function of the gray level respectively for these two orientations. We note that even when there is no time flicker, as when the applied voltage is below the threshold value at gray level zero, there are other phenomena producing depolarization such as diffraction or disclinations in the LC^{[6][11]}. They are generally negligible as we see in the high DOP value at zero gray level: 1.002 and 0.997 in Figs. 2(b) and (d).

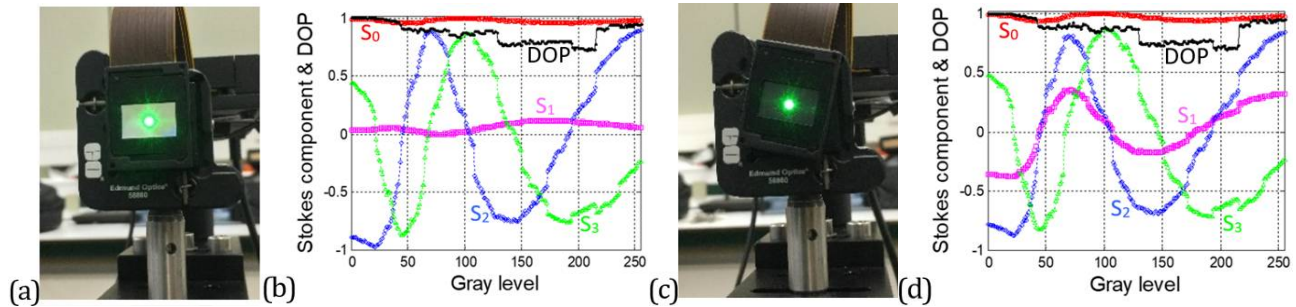


Fig. 2. LCoS images and experimental values for the Stokes parameters and DoP, for RHC as input SOP and $\lambda = 532$ nm: (a) and (b) for horizontal (i.e. unrotated) orientation; (c) and (d) for rotated orientation.

In Fig. 3(a) and (b) we show the resultant calibrated values, both for the horizontal and rotated orientations (in legend), given by Eqns. (4a) and (4b) respectively for the average retardance and its flicker amplitude as a function of gray level. According to the theory, these magnitudes should be invariant with the director orientation, which is verified in the results in Fig. 3. The voltage dynamic range is about 550° , that is larger than 360° , since for this work we wanted a large excursion to verify the validity of our approach. In Fig. 3(b) we show the flicker magnitude, which reaches values larger than 70° at about gray level 200. If we limit the step between V_b and V_d , then flicker is decreased along with the retardance range: for example, if only 360° are necessary, with this LCoS, we limit $V_b = 1.90$ V and then the maximum flicker decreases to about 40° .

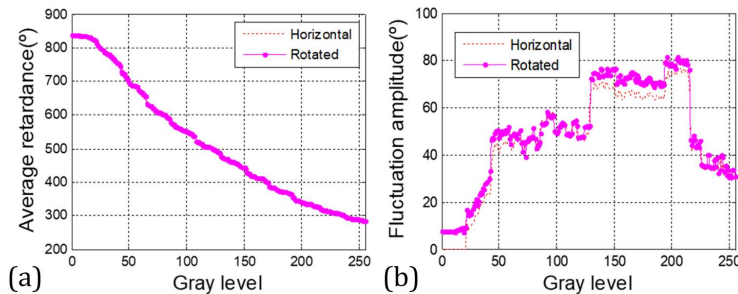


Fig. 3. For $\lambda = 532$ nm, calibrated values for the horizontal and rotated cases (in legend) for: (a) average retardance; (b) flicker.

In Fig. 4 we show the results for the LC-director orientation and for the two cases (in the legend). In Fig. 4(a) the results are shown with respect to the average retardance, related to the gray level by Fig. 3(a). The dotted lines are the “raw” results given by the direct application of Eq. (4c) and the round symbol plots result from the interpolation using the calibrated values in the ranges where Eq. (4c) is robust, since at points $\bar{\Gamma} = m 180^\circ$ we get an indetermination. What we do is to consider only the calibrated points where $\bar{\Gamma} = 90^\circ + m 180^\circ$, with m an integer, and a range $\pm 60^\circ$ about these points. And using this robust ranges we obtain a cubic interpolating function, the round symbol lines in Fig. 4(a). We see that the LC-director orientation at low gray levels (large retardance) is about 0° and 12.3° for the unrotated and rotated cases, which are the values obtained with the crossed polarizers technique when the LCoS is switched-off. Then, we see that the orientation changes with the retardance, i.e. with the applied voltage, with the unrotated and rotated curves running

almost in parallel. To better appreciate this variation in the LC-director orientation with the applied voltage, we produce Fig. 4(b), where the interpolating curves for both orientations are represented as a function of the gray level and centered around their respective average values. We see that the curves show very similar variations with a range of 6.9° for the horizontal and 6.1° for the rotated.

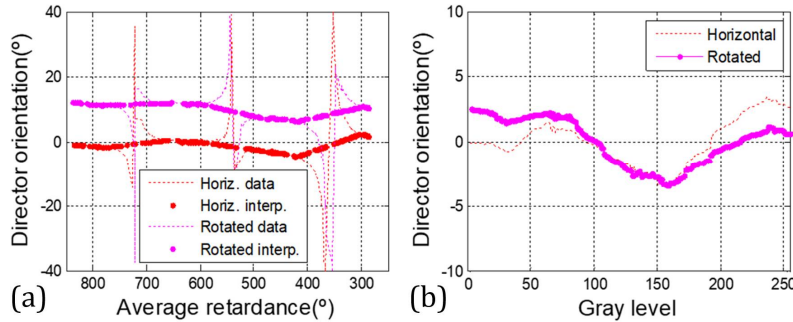


Fig. 4. For $\lambda = 532$ nm, calibrated values for the horizontal and rotated cases (in legend) for the director orientation: (a) “raw” and interpolated curve; (b) interpolated curve with the average value subtracted.

The reason for this LC-director changes with the applied voltage are not clear. Something that we need to note is that, as we have shown in Eq. (1), any unitary device in reflection is equivalent to a rotated linear retarder. Then, one possibility is that the increase of voltage not only produces a tilt of the molecules in the bulk of the LC layer but it also adds some residual out of plane tilt, i.e. a residual twist, which is globally reflected as a rotated LC-director. Other options might also be compatible with this behavior. The analysis of the possible causes is being studied through rigorous numerical modelling^[19].

4.2. Prediction capability

Now, we are interested in studying if our approach enables accurate prediction of the modulation capabilities of the LCoS device. To this goal we will show the comparison between simulation and experimental measurements for two different kinds of experiments. On one side, when the magnitude of interest is the state of polarization of the output light which is useful for generation of polarization structured light beams^{[20][21]}. On the other side when we are interested in the intensity transmission.

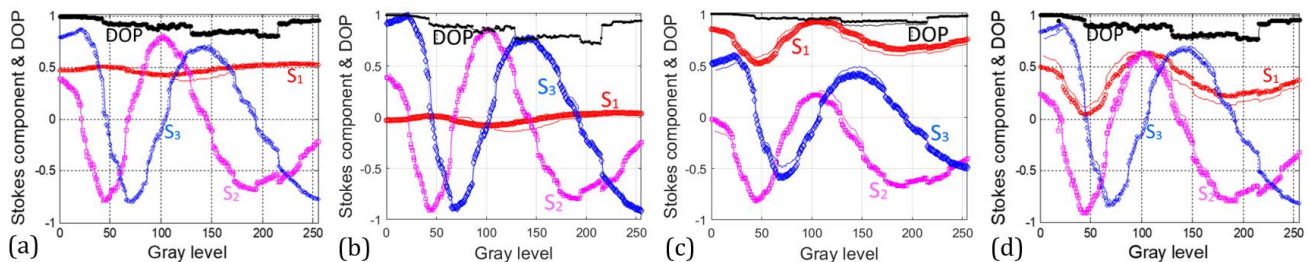


Fig. 5. Polarimetric predictions using $\lambda = 532$ nm and comparing experimental (dots) and simulated (continuous lines) values, for the horizontal and rotated cases for the director orientation: for the horizontal case and input SOP linearly polarized at 30° (a) and at 45° (b); for the rotated case and input SOP linearly polarized at 28° (c) and 43° . (d)

In Fig. 5 we show that the calibration can be applied to predict the reflected SOP across the whole gray level range for any possible input SOP. We show the Stokes components and DoP as a function of applied voltage for horizontal orientation and for input SOP linearly polarized at 30° and at 45° respectively in Fig. 5(a) and 5(b), and for rotated orientation and input SOP linearly polarized at 28° and at 43° respectively in Fig. 5(c) and 5(d). The circle symbol lines correspond to the experimental measurements and the continuous line corresponds to the predicted curve using the values for the calibrated parameters. We see that the agreement is very good in all the situations. We are even able to follow the jumps in the magnitudes, clearly visible in some part of the plots, which are due to the bitmap division of the signal that is being addressed to the LCoS device.

In the next plots we show the predictive capability of the proposed approach for calculation of the intensity transmission as a function of the applied voltage both for the horizontal and the rotated cases, respectively in Figs 6 and 7. In the caption there is the detailed description of the specific input and output orientations for the external polarization elements. The circle symbol lines correspond to the experimental measurements and the continuous line corresponds to the predicted curve using the values for the calibrated parameters. We see that the agreement is very good in all the situations as it also was in Fig. 5. Altogether demonstrates the excellent capabilities of the model and characterization approach presented.

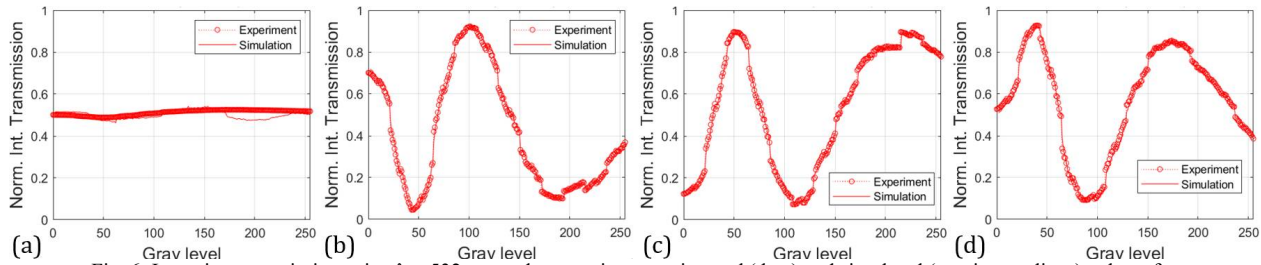


Fig. 6. Intensity transmission using $\lambda = 532$ nm and comparing experimental (dots) and simulated (continuous lines) values, for the horizontal case for the director orientation. We illuminate with RHC polarized light, and the analyzing system is composed of polarizer with its transmission axis at 0° preceded by a quarter waveplate at: (a) -90° ; (b) -45° ; (c) $+30^\circ$; (d) $+60^\circ$.

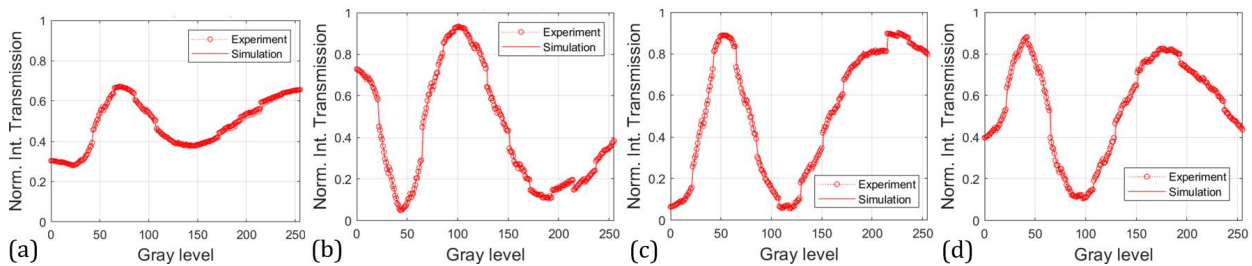


Fig. 7. Intensity transmission using $\lambda = 532$ nm and comparing experimental (dots) and simulated (continuous lines) values, for the rotated case for the director orientation. We illuminate with RHC polarized light, and the analyzing system is composed of polarizer with its transmission axis at 0° preceded by a quarter waveplate at: (a) -90° ; (b) -45° ; (c) $+30^\circ$; (d) $+60^\circ$.

5. CONCLUSIONS

We have demonstrated a novel approach, based on time-average Stokes polarimetry for the characterization of LCoS devices. The method enables to obtain the LC-director orientation, the average retardance and its flicker as a function of the applied voltage. We have shown that the experimental calibration setup is very simple, and the approach relies on analytic expressions, what makes it a technique easy to implement. We see that the director orientation changes across the voltage range, especially at larger gray levels. This is a small effect but in very sensitive phase-only applications will produce a coupling between amplitude and phase. It is also an interesting result which needs to be further investigated to learn what its origin can be, and probably can shed some light into internal dynamics in the LC layer. We have also shown that the approach is able to provide very accurate prediction in a wide range of situations, both for polarimetric applications and for intensity transmission experiments.

ACKNOWLEDGEMENTS

Ministerio de Ciencia e Innovación (Spain) (FIS2017-82919-R (MINECO/AEI/FEDER, UE); PID2019-106601RB-I00); Generalitat Valenciana (Spain) (GV/2019/021; CDEIGENT/2018/024); Universidad de Alicante (Spain) (UATALENTO18-10).

REFERENCES

- [1] Z. Zhang, Z. You, and D. Chu, "Fundamentals of phase-only liquid crystal on silicon (LCOS) devices," *Light Sci. Appl.* 3, 1-10 (2014).
- [2] G. Lazarev, P.-J. Chen, J. Strauss, N. Fontaine, A. Forbes, "Beyond the display: Phase-only liquid crystal on Silicon devices and their applications in photonics," *Opt. Express* 27, 16206–16249 (2019).
- [3] A. Márquez, A. Lizana, "Special Issue on Liquid Crystal on Silicon Devices: Modeling and Advanced Spatial Light Modulation Applications," *Appl. Sci.* 9, 3049 (2019).
- [4] A. Lizana, I. Moreno, A. Márquez, C. Iemmi, E. Fernández, J. Campos, and M. J. Yzuel, "Time fluctuations of the phase modulation in a liquid crystal on silicon display: characterization and effects in diffractive optics," *Opt. Express* 16, 16711 (2008).
- [5] R. Li and L. Cao, "Progress in Phase Calibration for Liquid Crystal Spatial Light Modulators," *Appl. Sci.* 9, 2012 (2019).
- [6] J. E. Wolfe and R. A. Chipman, "Polarimetric characterization of liquid-crystal-on-silicon panels," *Appl. Opt.* 45, 1688–1703 (2006).
- [7] C. Ramirez, B. Karakus, A. Lizana, and J. Campos, "Polarimetric method for liquid crystal displays characterization in presence of phase fluctuations," *Opt. Express* 21, 3182–3192 (2013).
- [8] F. J. Martínez, A. Márquez, S. Gallego, J. Francés, and I. Pascual, "Extended linear polarimeter to measure retardance and flicker: application to liquid crystal on silicon devices in two working geometries," *Opt. Eng.* 53, 014105 (2014).
- [9] F. J. Martínez, A. Márquez, S. Gallego, J. Francés, I. Pascual, and A. Beléndez, "Retardance and flicker modeling and characterization of electro-optic linear retarders by averaged Stokes polarimetry," *Opt. Lett.* 39, 1011–1014 (2014).
- [10] F. J. Martínez, A. Márquez, S. Gallego, M. Ortuño, J. Francés, A. Beléndez, and I. Pascual, "Averaged Stokes polarimetry applied to evaluate retardance and flicker in PA-LCoS devices," *Opt. Express* 22, 15064–15074 (2014).
- [11] A. Márquez, F. J. Martínez-Guardiola, J. Francés, S. Gallego, I. Pascual, and A. Beléndez, "Combining average molecular tilt and flicker for management of depolarized light in parallel-aligned liquid crystal devices for broadband and wide-angle illumination," *Opt. Express* 27, 5238 (2019).
- [12] H. Yang and D. P. Chu, "Phase flicker in liquid crystal on silicon devices," *J. Phys. Photonics* 2, 032001 (2020).
- [13] H. M. P. Chen, J. P. Yang, H. T. Yen, Z. N. Hsu, Y. Huang, and S. T. Wu, "Pursuing high quality phase-only liquid crystal on silicon (LCoS) devices," *Appl. Sci.* 8, (2018).
- [14] T. Lu, M. Pivnenko, B. Robertson, and D. Chu, "Pixel-level fringing-effect model to describe the phase profile and diffraction efficiency of a liquid crystal on silicon device," *Appl. Opt.* 54, 5903 (2015).
- [15] A. Márquez, F. J. Martínez-Guardiola, J. Francés, E. M. Calzado, D. Puerto, S. Gallego, I. Pascual, and A. Beléndez, "Unitary matrix approach for a precise voltage dependent characterization of reflective liquid crystal devices by average Stokes polarimetry," *Opt. Lett.* 45, 5732-5735 (2020).
- [16] C. R. Fernández-Pousa, I. Moreno, N. Bennis, and C. Gómez-Reino, "Generalized formulation and symmetry properties of reciprocal nonabsorbing polarization devices: application to liquid-crystal displays," *J. Opt. Soc. Am. A* 17, 2074 (2000).
- [17] A. Márquez, I. Moreno, J. Campos, and M. J. Yzuel, "Analysis of Fabry-Perot interference effects on the modulation properties of liquid crystal displays," *Opt. Commun.* 265, 84–94 (2006).
- [18] D. Goldstein, *Polarized Light*, 2nd Edition (Marcel Dekker, 2003).
- [19] P. Yeh and C. Gu, *Optics of Liquid Crystal Displays*, 2nd ed. (John Wiley & Sons Inc., 2009).
- [20] T. G. Brown, Q. Zhan, "Focus Issue: Unconventional Polarization States of Light," *Opt. Express* 18, 10775-10776 (2010).
- [21] X. Zheng, A. Lizana, A. Peinado, C. Ramirez, J. L. Martinez, A. Marquez, I. Moreno, and J. Campos, "Compact LCOS-SLM based polarization pattern beam generator," *J. Lightwave Technol.* 33, 2047-2055 (2015).